In this new setup, the current flowing across the Pt100/polysilicon resistor (green line in Figure 142) was not monitored through a PC-DAC input as before (see p.157), but forced instead using a precision ultralow offset voltage (25 μV) OP07-EP operational amplifier (*Analog Devices*). In essence, a very stable 10 V voltage (±25 mV) was obtained from a precision REF102 voltage reference (*Burr-Brown*). A 10 kΩ 0.1% precision resistor was then placed in the current path to force a 1 mA current through the sensing element. Instead of monitoring the passing current, the ground source of the voltage reference was connected to he negative input of an OP07 operational amplifier arranged in a voltage-follower configuration, whilst the positive input was linked to the load resistor end. The virtual-ground principle governing op-amp inputs ensured that the voltage at the load resistor end had to be the same as that of the voltage reference ground source or, in other words, that the voltage falling across the load resistor had to be exactly 10 V. This meant that the current flowing across the resistor (and therefore across the sensing element) had to be a 1 mA current, without regard of a small drift from build-up heating in the load resistor that could be easily software-compensated during calibration. As before, the voltage drop across the sensing element was monitored with an INA114 precision differential amplifier (*Burr-Brown*), set at a 34.47 gain using a 1.49 kΩ resistor. With this setup, the resistance of the Pt100/polysilicon resistor could be easily evaluated in terms of the read voltage and the forced current:

$$R_S = \frac{V_R}{0.001 \cdot 34.47} \cdot C_C \quad \Rightarrow \quad R_S = V_R \cdot 29.0107 \cdot C_C$$

Equation 11 - Sensing element resistance (R_S) as a function of the read voltage (V_R). C_C is a linear software-calibration constant for adjusting the INA114 gain and compensating small load resistor voltage drifts.

The new dual-acquisition circuit replaced the old Pt100 conditioning circuitry and also acted as a "bridge" between driver and thermocouple circuits and the PC-DAC. Since more analog inputs were available in NRSE mode, the analog multiplexer previously used to switch between driver consumption voltages was removed, offering a more precise reading of the driver power consumption through direct voltage measurement. The schematic view of the complete circuitry setup can be observed in Figure 143. Again, all modules (with the exception of the driver module) were

inserted in RF-shielding boxes, and all signal paths were shielded with grounded metallic wire meshes.
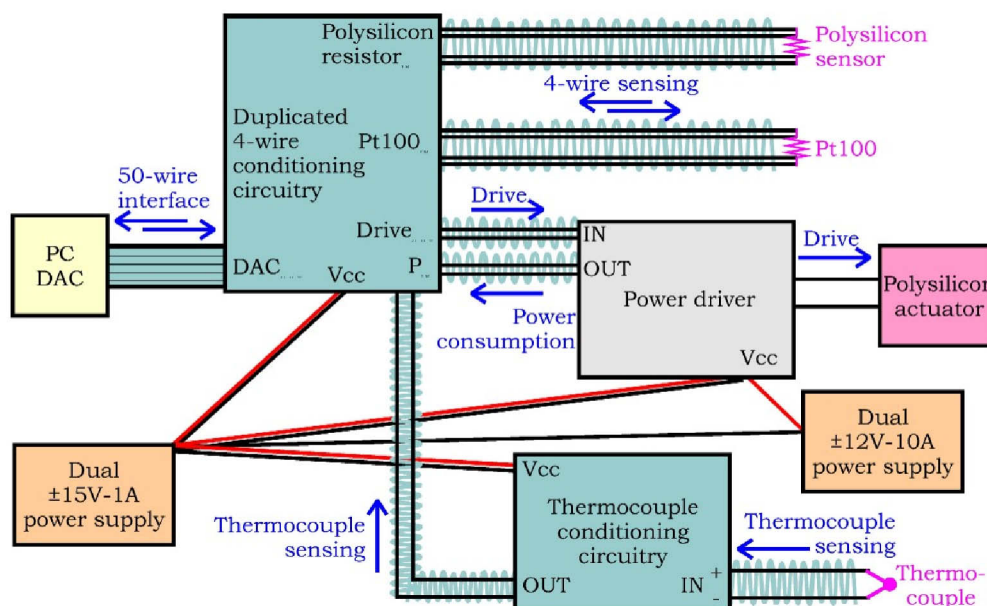

Figure 143 - Basic interconnection scheme for the new conditioning circuitry setup. As before (see p.159), the ground source is distributed in a radial manner to minimize ground-loop errors.

Sensor calibration

The first step in sensor calibration, having replaced the Pt100 conditioning circuitry, was to recalibrate the Pt100 sensor in de-ionized water, as described previously (see p.157, *Materials and Methods*, p.310). After Pt100 recalibration, the polysilicon resistor sensors were calibrated by immersion in mineral oil (to avoid any superficial current leakages on the chip) on a hotplate-stirrer, together with the Pt100 and thermocouple inboard sensors, and an external thermocouple sensor for cross-reference (see *Materials and Methods,* p.312 for details).

As in the case of bare polysilicon chips (see p. 231), calibration data (see Figure 144a) revealed an extremely linear behavior of polysilicon resistors over the PCR temperature range (40-100 °C), as can be gauged from the very small deviation between linear and third-order polynomial fits (see Figure 144b). Calibration results also confirmed the suspicion that the previously measured high TCR (see p.231) was a numerical artifact arising from the use of very small sensor resistors (4-6 Ω). The new data for ~100 Ω resistors suggested a much smaller (~$9.05\cdot10^{-4}$ °C^{-1}) TCR, but still far larger

than that predicted by simulations (~$4.34 \cdot 10^{-4}$ °C^{-1}). Calibration results for A and B wafer chips gave similar results ($1.12 \cdot 10^{-3}$ and $6.38 \cdot 10^{-4}$ °C^{-1} respectively).
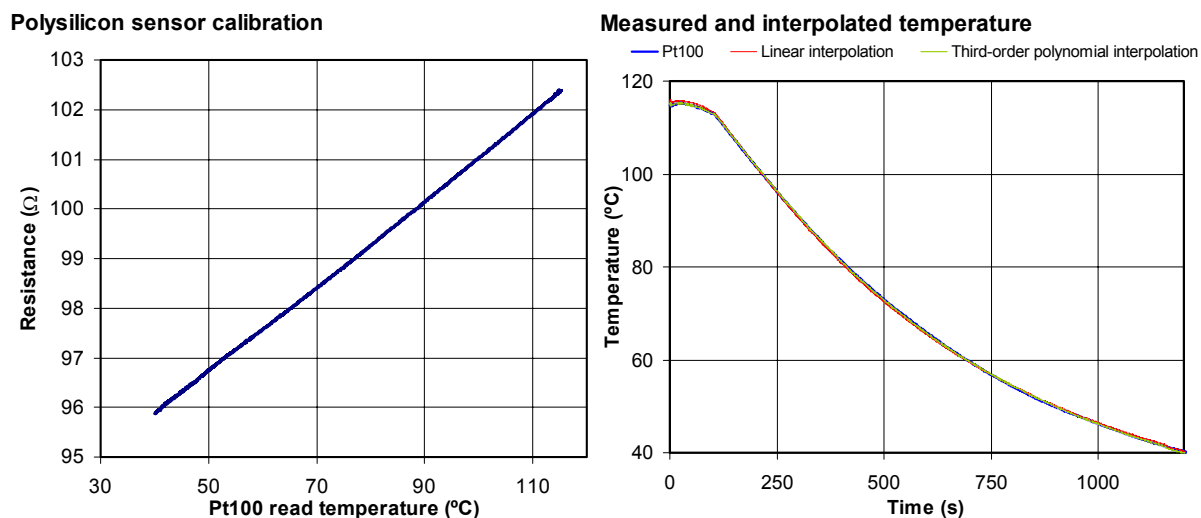
Polysilicon sensor calibration

Measured and interpolated temperature

Figure 144 - Temperature fall (120→40 °C) calibration data (a) and interpolated temperature (b) for a wafer-C polysilicon sensor. Mean deviation of third-order polynomial interpolated temperature: 0.2 °C.

Sensor/actuator functional tests

In order to functionally test the dual sensor-actuator behavior of active PCR chips, systematic calibration was conducted for three rhomboidal and three serpentine-like chips (mainly wafer-B chips), and their third-order interpolation curves were stored in the control software for later real-time LUT operation (see *Materials and Methods*, p.314).

Ground loops

Initial operation assays were conducted with a clamped Pt100 sensor, in order to verify temperature cycling accuracy and to evaluate any existing differences in thermal behavior between sensors. Results, as those shown in Figure 145, indicated that a coupling effect of some kind was taking place, linking actuator thrust and sensor input in a non-linear manner.
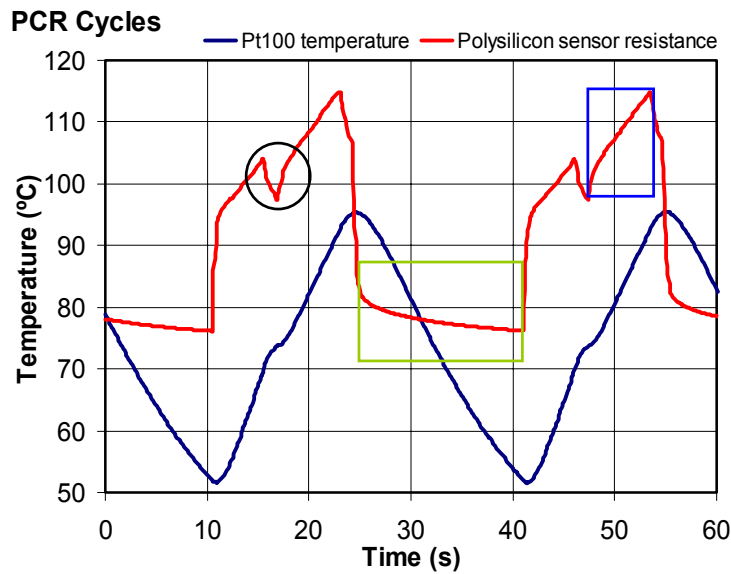
Figure 145 - Non-linear, drive-thrust dependent behavior on the measured sensor resistance during a 95 °C - 0 s → 53 °C - 0 s → 72 °C - 0 s cycle. Two different slopes (green and blue boxes) can be distinctly observed during cooling (no actuator current) and heating periods, with punctuated transitions in between. The current-dependant effect is most marked at 72 °C (black circle), where thrust is just momentarily switched off, showing no acute effect on Pt100 behavior, but an abrupt discontinuity in polysilicon sensor resistance.

Although the current-dependant behavior of polysilicon resistors shown in Figure 145 could indeed have been modeled to some extent, this was not deemed a safe policy when aiming at providing precision temperature measurements for PCR operation and, therefore, steps were taken to mitigate or eradicate the problem. Different explanations, such as capacitive coupling or fast direct heat radiation could partly explain the observed phenomenon, but they were judged untenable for several reasons. On the one hand, capacitive coupling should not be a noticeable effect in DC circuits, and the transitional operations on drive current were not considered fast enough to account for such effects. On the other hand, direct infrared radiation between sensor and actuator grids (i.e. thermal coupling) could explain different heating/cooling slopes, and even (if considered a noticeable effect) a thermal, gap-like offset between Pt100 and polysilicon measures when switching on thrust, but it should not account for the observed saltations when power was switched off. Therefore, even though ground-loop effects had theoretically been addressed by radially distributing the ground source, steps were taken to discard them as the inherent cause of the observed non-linearity in polysilicon sensor behavior.